NANOSYSTEMS:
PHYSICS, CHEMISTRY, MATHEMATICS

Elovikov D.P., et al. *Nanosystems: Phys. Chem. Math.*, 2022, **13** (6), 662–667.
http://nanojournal.ifmo.ru
DOI 10.17586/2220-8054-2022-13-6-662-667

Original article

Thermal stability of the waylandite-structured nanocrystalline $BiAl_3(PO_4)_2(OH)_6$

Dmitry P. Elovikov[1,2,a], Olga V. Proskurina[1,3,b], Maria V. Tomkovich[1,c], Valery L. Ugolkov[4,d], Victor V. Gusarov[1,e]

[1]Ioffe Institute, St. Petersburg, Russia

[2]St. Petersburg Electrotechnical University "LETI", St. Petersburg, Russia

[3]St. Petersburg State Institute of Technology, St. Petersburg, Russia

[4]I. V. Grebenshchikov Institute of Silicate Chemistry of the Russian Academy of Sciences, St. Petersburg, Russia

[a]syncdima@mail.ru, [b]proskurinaov@mail.ru, [c]maria.tom83@gmail.com, [d]ugolkov.52@gmail.com, [e]victor.v.gusarov@gmail.com

Corresponding author: Dmitry P. Elovikov, syncdima@mail.ru

ABSTRACT A nanocrystalline powder of the waylandite-structured bismuth hydroaluminophosphate was obtained under hydrothermal conditions at 200 °C, 7 MPa and pH 7, and characterized by X-ray diffractometry, scanning electron microscopy (SEM), and energy dispersive microanalysis (EDAX). The simultaneous thermal analysis and high-temperature X-ray diffractometry have shown that the crystal-chemical formula of this compound can be represented as $BiAl_3(PO_4)_2O(OH)_4 \cdot (H_2O)$. This compound retains its structure and crystallite size (∼65 nm) up to about 500 °C. It has been determined that the decomposition of this compound in the 540–800 °C range results in the formation of Bi_2O_3, $Bi_2Al_4O_9$ and $AlPO_4$ phases. At temperatures above 800 °C, a complete thermal decomposition of $Bi_2Al_4O_9$ and the formation of crystalline α-Al_2O_3 occur in this system, while Bi_2O_3 keeps evaporating during the isothermal exposure.

KEYWORDS nanocrystals, waylandite-structured, $BiAl_3(PO_4)_2O(OH)_4 \cdot (H_2O)$, thermal stability, hydrothermal synthesis, nature-like technologies.

ACKNOWLEDGEMENTS X-ray diffraction studies and elemental analyses of samples were performed employing the equipment of the Engineering Center of the St. Petersburg State Institute of Technology (Technical University). The research was supported by the Russian Science Foundation Grant 21-13-00260

FOR CITATION Elovikov D.P., Proskurina O.V., Tomkovich M.V., Ugolkov V.L., Gusarov V.V. Thermal stability of the waylandite-structured nanocrystalline $BiAl_3(PO_4)_2(OH)_6$. *Nanosystems: Phys. Chem. Math.*, 2022, **13** (6), 662–667.

1. Introduction

In recent years, there has been an active interest in the development of new functional materials based on synthetic minerals and of their technologies (nature-like technologies). Such interest is primarily due to the possibility of obtaining new materials with unique properties [1–3].

Phosphates of the alunite supergroup are an extensive class of inorganic compounds with the $AB_3(PO_4)_2(OH)_6$ chemical formula, where A is Ce, La, Nb, Sm, Ca, Sr, Pb, Ba, Bi, and B is Al, Fe, V; they are similar in their structural parameters, syngony (trigonal/hexagonal), space group ($R\bar{3}m$), and represent crystals with the hexagonal scalenohedron geometry [4–10].

The relevance of obtaining and studying such phosphates, in particular, lies in the prospects of using them as matrices for toxic and radioactive waste due to their structural features, thermal stability and high ability to ionic substitution of toxic Hg, As, Tl, Sb, Cr, Ni, Ca, radioactive K, Sr, Th, U, Ra, Pb and rare earths [10–14]. Data on the synthesis of these compounds are scanty and have a number of shortcomings. This is determined by the fact that the preparation of such compounds is complicated by the long duration of crystalline phases formation, from two weeks to six months [11, 12, 15, 16]. It should be noted that in some of the listed works the performed synthesis used natural minerals and yielded mixtures of phases rather than individual compounds. The mentioned works contain no data on the kinetics and mechanisms of compounds formation.

The study of the thermal behavior of phases is of fundamental scientific interest. An analysis of the literature on the thermal stability of phosphates of the alunite supergroup showed the paucity of the available data [12, 15, 17, 18]. In most scientific works, the objects of study are natural minerals which contain impurity components and are phases of variable composition. Phosphates of the alunite supergroup tend to include impurity cations and anions from the environment

into their structure, which affects the results of studying their properties. There are no data on the study of individual compounds.

To obtain hydroxide and oxide phases, methods of hydrothermal, hydrothermal-microwave and hydrothermal-ultrasonic treatment [19–24] are widely used. Hydrothermal synthesis has produced many artificial analogs of minerals [25–30] positively differing from natural ones by the strictly defined composition and morphology, and prescribed size distribution of particles. An analysis of the currently available scientific literature has shown that the waylandite-structured $BiAl_3(PO_4)_2(OH)_6$ crystalline phase was successfully obtained for the first time under hydrothermal conditions [31].

There is no information on the thermal stability and thermal behavior of the $BiAl_3(PO_4)_2(OH)_6$ compound. In this regard, the present work is aimed at studying the thermal stability of the waylandite-structured nanocrystalline $BiAl_3(PO_4)_2(OH)_6$.

2. Experimental

To obtain waylandite-structured nanocrystalline $BiAl_3(PO_4)_2(OH)_6$ under hydrothermal conditions, the following reagents were used: $Bi(NO_3)_3{\cdot}5H_2O$ (p.a.), $Al(NO_3)_3{\cdot}9H2O$ (puriss.), $(NH_4)_2HPO_4$ (p.a.), HNO_3 (puriss. spec.), and NaOH (puriss.). Bismuth and aluminum nitrate samples, calculated to obtain $BiAl_3(PO_4)_2(OH)_6$, were dissolved in 6 M aqueous HNO_3 solution with stirring until complete dissolution. An aqueous solution of $(NH_4)_2HPO_4$ prepared by dissolving a sample calculated according to stoichiometry in distilled water, was added dropwise to the resulting solution. Next, a 4 M aqueous NaOH solution was added dropwise to the resulting suspension with stirring, until pH 7 was reached.

Hydrothermal treatment of suspensions was carried out in steel autoclaves with Teflon chambers at 200 °C and a pressure of 7 MPa for 12 days in a hydrothermal fluid at pH=7. The resulting precipitate was separated by centrifugation, rinsed with distilled water until neutral, and dried at 80 °C for 6 hours.

The determination of the morphology and particle size, and of elemental composition of the samples was carried out by scanning electron microscopy (SEM) and energy dispersive microanalysis (EDAX) using a Tescan Vega 3 SBH electron microscope (TESCAN Brno, Czech Republic) with an Inca X-Act elemental analysis attachment (Oxford Instruments plc, Great Britain).

X-ray diffraction measurements of the powder sample were carried out on a Rigaku SmartLab 3 diffractometer (Rigaku, Japan), equipped with an X-ray tube with a copper anode, in the Bragg-Brentano geometry. CuK_α doublet radiation was monochromatized using a nickel K_β filter. The shooting was carried out in air at a constant temperature of 25 °C. The size of the crystallites was calculated by the Hall method for peaks $10\bar{1}1$, $11\bar{2}0$, $11\bar{2}3$, $02\bar{2}4$ and $30\bar{3}3$.

The high-temperature X-ray diffraction analysis of the powder sample was carried out on an XRD-7000 diffractometer (Shimadzu, Japan) with an HTK 1200 N high-temperature attachment (Anton Paar, Austria).

Possible crystalline phases were identified using PDF-2 (Powder Diffraction File-2) [32] and Crystallography Open Database [33] powder databases.

The simultaneous thermal analysis coupled with mass spectrometry for the analysis of evolved gases employed an STA 429 CD in combination with a QMS 403 C (NETZSCH, Germany) quadrupole mass spectrometer with a heating rate of 10 °C/min from 25 to 950 °C.

3. Results and discussion

Thermal studies were carried out on powdered nanocrystalline $BiAl_3(PO_4)_2(OH)_6$ obtained by hydrothermal synthesis at pH 7. The elemental analysis showed that the bismuth, aluminum and phosphorus ratio in the initial samples corresponds to the stoichiometry of the individual $BiAl_3(PO_4)_2(OH)_6$ compound with an error in determining the elemental composition up to 5 at. %. All peaks in the X-ray diffraction pattern (Fig. 1) correspond to the waylandite-structured $BiAl_3(PO_4)_2(OH)_6$ [31]. The crystallite size is ∼65 nm.

According to the SEM data presented in Fig. 2, it can be seen that the compound particles after synthesis are represented by rod-like aggregates composed by smaller particles. At heating the sample up to 1000 °C, the particle morphology changes only slightly, while the heating to temperatures above 1000 °C leads to a sharp change in particle morphology (Fig. 2).

According to the simultaneous thermal analysis data using mass spectrometry, four areas of water release from the sample can be noted (Fig. 3).

The first region (80–318 °C), characterized by a loss of ∼1 wt. %, is associated with the removal of the adsorbed water from the sample. The second region (318–498 °C), characterized by a loss of ∼3.5 wt. % of water, is associated with an endothermic effect that is well pronounced in the thermogram and can be associated with the removal of a part of water from the $BiAl_3(PO_4)_2(OH)_6$ compound. At the same time, according to the X-ray diffraction data, the initial structure of waylandite does not undergo any changes (Fig. 4). Consequently, it would be apparently more correct to represent the crystal-chemical formula of this compound as $BiAl_3(PO_4)_2(OH)_4{\cdot}(H_2O)$. In this regard, this formula is similar to that adopted for the $CaAl_3(PO_4)_2(OH)_5{\cdot}(H_2O)$ compound with a similar structure [17]. The third (498–597 °C) and fourth (597–600 °C) regions, which are difficult to separate from each other according to thermogravimetric data and the results of differential thermal analysis, and are characterized by a weight loss of ∼3.2 and ∼2.4 wt. %, respectively, are associated with the process of $BiAl_3(PO_4)_2(OH)_4{\cdot}(H_2O)$ dehydroxylation. In this case, sample amorphization occurs

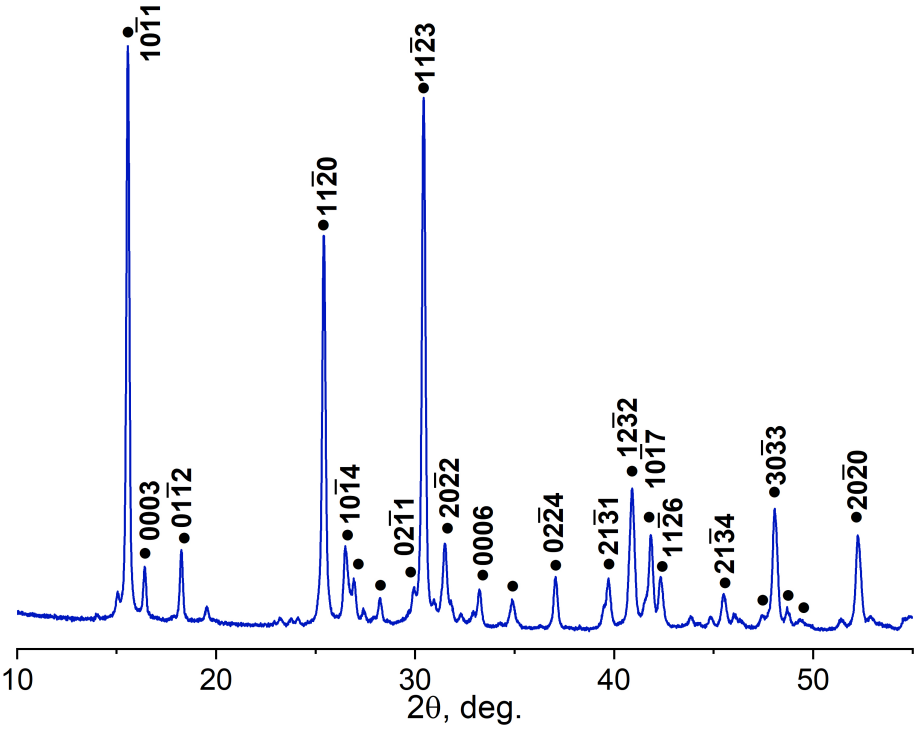

FIG. 1. X-ray diffraction pattern of $BiAl_3(PO_4)_2(OH)_6$ synthesized under hydrothermal conditions. The X-ray diffraction pattern shows the Miller–Brave (*hkil*) indices of the most intense peaks of the waylandite-structured compound

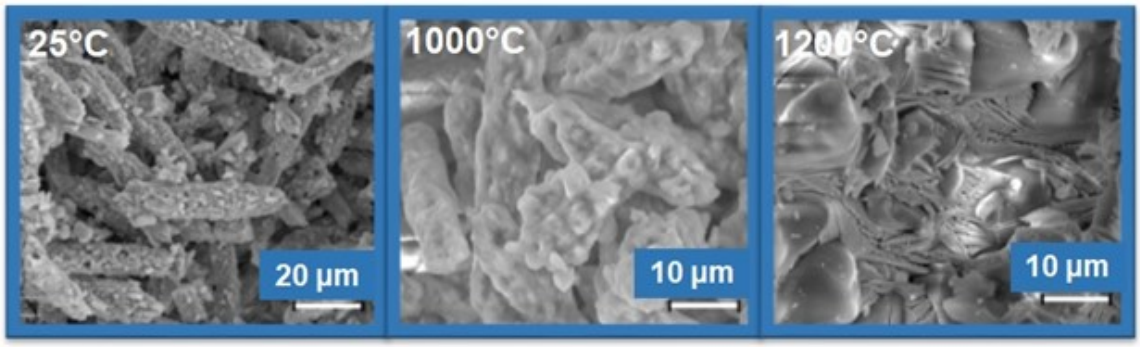

FIG. 2. SEM images of samples before and after heat treatment at 1000 and 1200°C

after the removal of all water from it. According to the calculation of the mass loss by the sample, each of the regions Nos. 2, 3, and 4 (Fig. 3) accounts for the removal of one H_2O molecule per $BiAl_3(PO_4)_2(OH)_4{\cdot}(H_2O)$ formula.

Thus, the above-described processes of stepwise separation of water from the compound can be represented as follows:

$$318\text{–}498\ ^\circ\text{C}: \quad BiAl_3(PO_4)_2O(OH)_4 \cdot H_2O \rightarrow BiAl_3(PO_4)_2O(OH)_4 + H_2O$$
$$498\text{–}597\ ^\circ\text{C}: \quad BiAl_3(PO_4)_2O(OH)_4 \rightarrow BiAl_3(PO_4)_2O_2(OH)_2 + H_2O$$
$$597\text{–}600\ ^\circ\text{C}: \quad BiAl_3(PO_4)_2O_2(OH)_2 \rightarrow [0.5Bi_2O_3 \cdot 1.5Al_2O_3 \cdot P_2O_5] + H_2O$$

It should be noted that the presented scheme suggests that a possibly metastable $BiAl_3(PO_4)_2O_2(OH)_2$ phase exists in a very narrow temperature range (about 597 °C).

According to high-temperature X-ray diffraction data, the onset of decomposition of the waylandite-structured phase with the appearance of peaks of the $Bi_2Al_4O_9$ phase, is observed at temperatures of about 500 °C (Fig. 4). During the isothermal exposure of the sample at 540 °C for about 30 min, peaks of the waylandite-structured phase are already weakly expressed in the diffraction pattern, and the appearance of trace amounts of crystalline $AlPO_4$ can be noticed in addition to peaks of the $Bi_2Al_4O_9$ phase (Fig. 4). Some temperature shift of phase transformation effects to lower temperatures according to high-temperature diffraction data compared to the data of simultaneous thermal analysis, is explained by the difference in sample heating conditions. The higher temperatures of the effects recorded by the simultaneous thermal

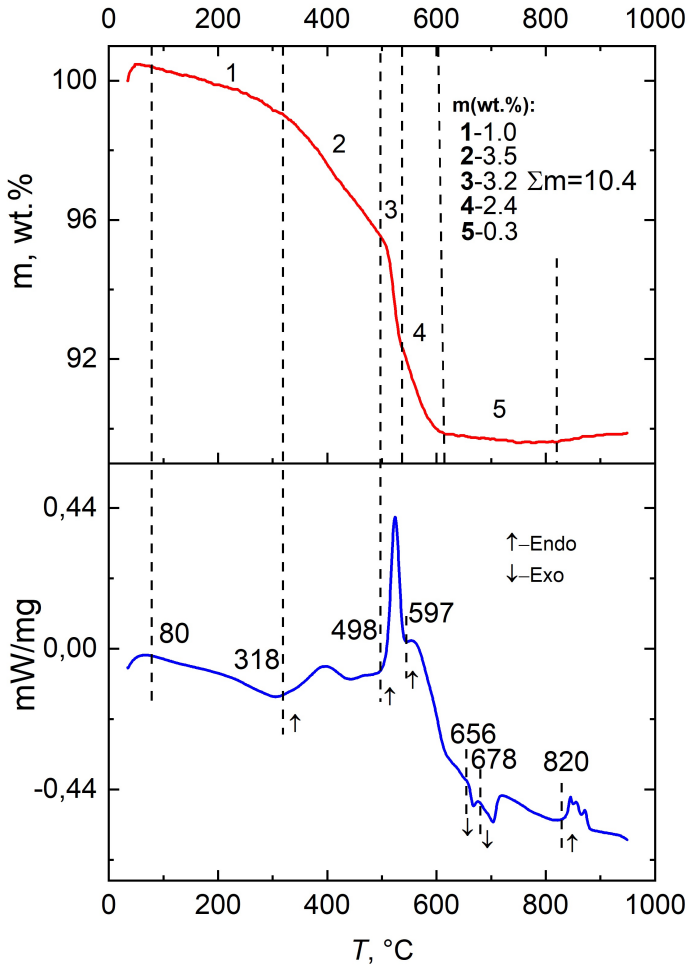

FIG. 3. Simultaneous thermal analysis data for the nanocrystalline $BiAl_3(PO_4)_2(OH)_6$ synthesized under hydrothermal conditions

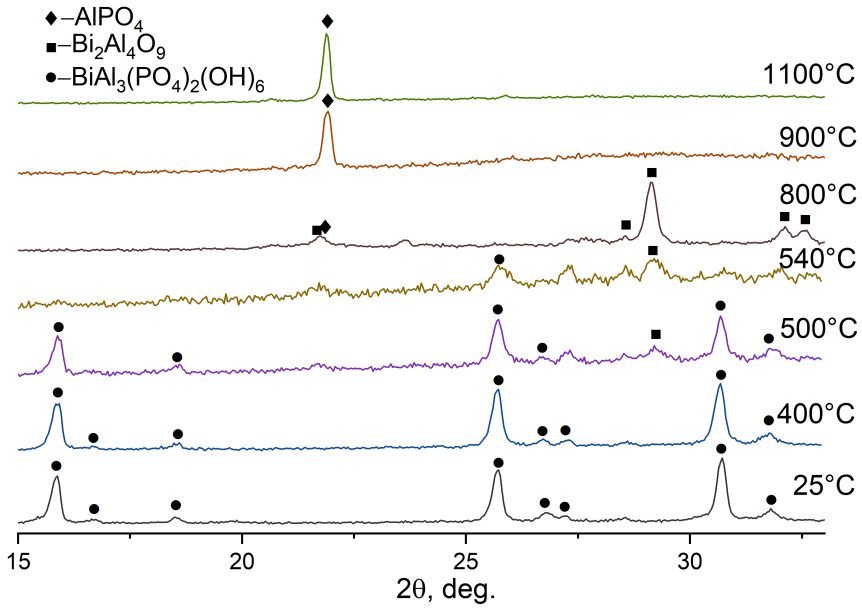

FIG. 4. High-temperature X-Ray diffraction data for the nanocrystalline $BiAl_3(PO_4)_2O(OH)_4 \cdot (H_2O)$ obtained under hydrothermal conditions.

analysis, are explained by the thermal inertia of the system, which always manifests itself under conditions of a constant heating rate [34, 35] of the samples. The exothermic peaks in the 656–720 °C temperature range noticed in the DTA curve (Fig. 3) are apparently associated with crystallization of the $Bi_2Al_4O_9$-, Bi_2O_3- and $AlPO_4$-based phases from the amorphous phase that formed during $BiAl_3(PO_4)_2(OH)_4 \cdot (H_2O)$ dehydration. According to high-temperature X-ray diffraction data, the process of crystallization of these phases can be considered almost complete at a temperature of about 800 °C (Fig. 4). Endothermic peaks in the 810–885 °C range in the DTA curve (Fig. 3) are associated, as can be concluded from the literature data [36–38], with the processes of eutectic phase melting and, possibly, phase transitions in the Bi_2O_3–Al_2O_3–P_2O_5 system.

It should be noted that according to the data on the broadening of X-ray diffraction lines, the sizes of crystallites in the waylandite-structured phase remain at a level of ∼65 nm within the entire temperature range of its existence (25–500 °C).

An analysis of high-temperature X-ray diffraction data (Fig. 3) and elemental analysis of the samples, which showed a sharp decrease in the bismuth content at processing temperatures above 900 °C, evidence that bismuth aluminate $Bi_2Al_4O_9$ decomposition at these temperatures is accompanied by melting and evaporation of bismuth oxide Bi_2O_3, which is consistent with the data from phase diagrams [36–38].

4. Conclusions

It has been shown that rod-like particles, which are aggregates of nanocrystals based on a waylandite-structured phase, form under hydrothermal conditions at pH 7. The crystal-chemical formula of the corresponding compounds can be represented as $BiAl_3(PO_4)_2O(OH)_4 \cdot (H_2O)$. It has been established that the structure of this compound is thermally stable up to about 500 °C, despite the fact that partial dehydration of the compound and formation of $BiAl_3(PO_4)_2O(OH)_4$ take place in the temperature range of about 300–500 °C. The size of phase crystallites remains at a level of about 65 nm in the temperature range up to 500 °C. The complete dehydration of the compound with the formation of an amorphous phase occurs in the range of 500–600 °C. The heating up to 800 °C leads to the formation of a mixture of $AlPO_4$, Bi_2O_3, and $Bi_2Al_4O_9$ crystalline phases. An increase of the temperature up to 900 °C and above leads to the decomposition of bismuth aluminate $Bi_2Al_4O_9$ and the evaporation of bismuth oxide.

References

[1] Kotova O. New adsorbent materials on the base of minerals and industrial waste. *Materials Science and Engineering*, 2019, **613**(1), P. 012001.

[2] Wei L., Li Z., Ye G., Rietveld L.C, van Halem D. Comparative study of low-cost fluoride removal by layered double hydroxides, geopolymers, softening pellets and struvite. *Environmental Technology*, 2022, **43**(27), P. 4306–4314.

[3] McMillen C.D., Kolis J.W. Hydrothermal synthesis as a route to mineralogically-inspired structures. *Dalton Transactions*, 2016, **45**(7), P. 2772–2784.

[4] Mills S.J., Kampf A.R., Raudsepp M., Birch W.D. The crystal structure of waylandite from Wheal Remfry, Cornwall, United Kingdom. *Mineralogy and Petrology*, 2010, **100**(3), P. 249–253.

[5] Repina S.A., Popova V.I., Churin E.I., Belogub E.V., Khiller V.V. Florencite-(Sm)-(Sm,Nd)$Al_3(PO_4)_2(OH)_6$: A new mineral species of the alunite-jarosite group from the Subpolar Urals. *Geology of Ore Deposits*, 2011, **53**(7), P. 564–574.

[6] Mills S.J., Kampf A.R., Raudsepp M., Christy A.G. The crystal structure of Ga-rich plumbogummite from Tsumeb, Namibia. *Mineralogical Magazine*, 2009, **73**(5), P. 837–845.

[7] Blount A.M. The crystal structure of crandallite. *American Mineralogist*, 1974, **59**, P. 41–47.

[8] Bayliss P., Kolitsch U., Nickel E.H., Pring A. Alunite supergroup: recommended nomenclature. *Mineralogical Magazine*, 2010, **74**(5), P. 919–927.

[9] Kolitsch U. Tiekink E., Slade P., Taylor M.R., Pring A. Hinsdalite and plumbogummite, their atomic arrangements and disordered lead sites. *European Journal of Mineralogy*, 1999, **11**, P. 513–520.

[10] Kolitsch U., Pring A. Crystal chemistry of the crandallite, beudantite and alunite groups: a review and evaluation of the suitability as storage materials for toxic metals. *Journal of Mineralogical and Petrological Sciences*, 2001, **96**(2), P. 67–78.

[11] Monteagudo J.M., Duran A., Carmona M.S., Schwab R.G., Higueras P. Elimination of inorganic mercury from waste waters using crandallite-type compounds. *Journal of Chemical Technology & Biotechnology*, 2003, **78**(4), P. 399–405.

[12] Gilkes R.J. Synthesis, Properties, and Dehydroxylation of Members of the Crandallite-Goyazite Series. *Mineralogical Magazine*, 1983, **47**, P. 221–227.

[13] Monteagudo J.M., Duran A., Martin I.S., Schwab R.G. Treatment of aqueous solutions containing nickel using crandallite-type compounds. *Journal of Chemical Technology & Biotechnology*, 2005, **81**(3), P. 262–267.

[14] Owen D.N., Cook N.J., Rollog M., Ehrig K.J., Schmandt D.S., Ram R., Brugger J., Ciobanu C.L., Wade B., Guagliardo P. REE-, Sr-, Ca-aluminum-phosphate-sulfate minerals of the alunite supergroup and their role as hosts for radionuclides. *American Mineralogist*, 2019, **104**(12), P. 1806–1819.

[15] Hikichi Y., Ohsato H., Miyamoto M. Syntheses and thermal changes of plumbogummite-group phosphate minerals. *Journal of the Mineralogical Society of Japan*, 1989, **19**(2), P. 67. (in Japanese).

[16] Schwab R.G., Pimpl T., Schukow H., Stolle A., Breitinger D.K. Compounds of the crandallite-type: Synthesis, properties and thermodynamic data of pure crandallite and woodhouseite. *Neues Jahrbuch für Mineralogie – Monatshefte*, 2004, **9**, P. 385–409.

[17] Frost R.L., Palmer S.J., Pogson R.E. Thermal stability of crandallite $CaAl_3(PO_4)_2(OH)_5 \cdot (H_2O)$ A 'Cave' mineral from the Jenolan Caves. *Journal of Thermal Analysis and Calorimetry*, 2012, **107**(3), P. 905–909.

[18] Francisco E.A.B., Prochnow L.I., Motta de Toledo M.C., Ferrari V.C., de Jesus S.L. Thermal treatment of aluminous phosphates of the crandallite group and its effect on phosphorus solubility. *Sci. agric. (Piracicaba, Braz.)*, 2007, **64**(3), P. 269–274.

[19] Pozhidaeva O.V., Korytkova E.N., Romanov D.P., Gusarov V.V. Formation of ZrO_2 Nanocrystals in Hydrothermal Media of Various Chemical Compositions. *Russian Journal of General Chemistry*, 2002, **72**(6), P. 849–853.

[20] Filippova A.D., Rumyantsev A.A., Baranchikov A.E., Kolesnik I.V., Ivanova O.S., Efimov N.N., Khoroshilov A.V., Ivanov V.K. Hydrothermal Synthesis of γ-WO_3 and h-WO_3 Powders in the Presence of Citric Acid and Their Photoprotective Properties. *Russian Journal of Inorganic Chemistry*, 2022, **67**(6), P. 780–789.

[21] Meskin P.E., Gavrilov A.I., Maksimov V.D., Ivanov V.K., Churagulov B.P. Hydrothermal/microwave and hydrothermal/ultrasonic synthesis of nanocrystalline titania, zirconia, and hafnia. *Russian Journal of Inorganic Chemistry*, 2007, **52**(11), P. 1648–56.

[22] Bachina A.K., Almjasheva O.V., Popkov V.I. Formation of $ZrTiO_4$ under Hydrothermal Conditions. *Russian Journal of Inorganic Chemistry*, 2022, **67**(6), P. 830–838.

[23] Enikeeva M.O., Proskurina O.V., Danilovich. D.P., Gusarov V.V. Formation of nanocrystals based on equimolar mixture of lanthanum and yttrium orthophosphates under microwave-assisted hydrothermal synthesis. *Nanosyst.: Phys. Chem. Math.*, 2020, **11**(6), P. 705–715.

[24] Lomakin M.S., Proskurina O.V., Levin A.A., Sergeev A.A., Leonov A.A., Nevedomsky V.N., Voznesenskiy S.S. Pyrochlore Phase in the Bi_2O_3–Fe_2O_3–WO_3–(H_2O) System: its Formation by Hydrothermal-Microwave Synthesis and Optical Properties. *Russian Journal of Inorganic Chemistry*, 2022, **67**(6), P. 820–829.

[25] Nikolaev A.I., Gerasimova L.G, Maslova M.V., Shchukina E.S. Synthetic analogues of natural titanosilicate mesoporous minerals as potential functional materials. Synthesis and application. *IOP Conference Series: Materials Science and Engineering*, 2019, **704**(1), P. 012003.

[26] Enikeeva M.O., Kenges K.M., Proskurina O.V., Danilovich D.P., Gusarov V.V. Influence of Hydrothermal Treatment Conditions on the Formation of Lanthanum Orthophosphate Nanoparticles of Monazite Structure. *Russian Journal of Applied Chemistry*, 2020, **93**(4), P. 540–548.

[27] Khrapova E.K., Kozlov D.A., Krasilin A.A. Hydrothermal Synthesis of Hydrosilicate Nanoscrolls $(Mg_{1-x}\ Co_x)_3Si_2O_5(OH)_4$ in a Na_2SO_3 Solution. *Russian Journal of Inorganic Chemistry*, 2022, **67**(6), P. 839–849.

[28] Gavryushkin P.N., Thomas V.G., Bolotina N.B., Bakakin V.V., Golovin A.V., Seryotkon Y.V., Fursenko D.A., Litasov K.D. Hydrothermal Synthesis and Structure Solution of $Na_2Ca(CO_3)_2$: "Synthetic Analogue" of Mineral Nyerereite. *Crystal Growth & Design*, 2016, **16**(4), P. 1893–1902.

[29] Thomas V.G., Demin S.P., Foursenko D.A., Bekker T.B. Pulsation processes at hydrothermal crystal growth (beryl as example). *Journal of Crystal Growth*, 1999, **206**(3), P. 203–214.

[30] Korytkova E.N., Pivovarova, L.N., Drosdova I.A., Gusarov V.V. Hydrothermal synthesis of nanotubular Co-Mg hydrosilicates with the chrysotile structure. *Russian Journal of General Chemistry*, 2007, **77**(10), P. 1669–1676.

[31] Elovikov D.P., Tomkovich M.V., Levin A.A., Proskurina O.V. Formation of the $BiAl_3(PO_4)_2(OH)_6$ Compound with a Waylandite Structure under Hydrothermal Conditions. *Russian Journal of Inorganic Chemistry*, 2022, **67**(6), P. 850–860.

[32] Fawcett T.G., Kabekkodu S.N., Blanton J.R., Blanton, T.N. Chemical analysis by diffraction: the Powder Diffraction File. *Powder Diffraction*, 2017, **32**(2), P. 63–71.

[33] Gražulis S., Merkys A., Vaitkus A. Crystallography Open Database (COD) W., Yip, S. (eds) Handbook of Materials Modeling. Springer, Cham. In: Andreoni, 2020, 1863 p.

[34] Šesták J. Dynamic Character of Thermal Analysis Where Thermal Inertia Is a Real and Not Negligible Effect Influencing the Evaluation of Non-Isothermal Kinetics: A Review. *Thermo*, 2021, **1**(2), P. 220–231.

[35] Holba P., Šesták J. Heat inertia and its role in thermal analysis. *Journal of Thermal Analysis and Calorimetry*, 2015, **121**(1), P. 303–307.

[36] Speranskaya E.I., Skorikov V.M., Safronov G.M., Gaidukov E.N. System Al_2O_3-Bi_2O_3. *Inorganic Materials*, 1970, **6**(7), P. 1201–1202.

[37] Oudich F., David N., Mathieu S., Vilasi M. Phase equilibria investigations and thermodynamic modeling of the system Bi_2O_3–Al_2O_3. *Journal of Nuclear Materials*, 2015, **457**, P. 72–79.

[38] Levin E.M., Roth R.S. Polymorphism of Bismuth Sesquioxide. II. Effect of Oxide Additions on the Polymorphism of Bi_2O_3. *Journal of Research of the National Bureau of Standards. Section A*, 1964, **68**(2), P. 197–206.

Submitted 29 August 2022; accepted 17 October 2022

Information about the authors:

Dmitry P. Elovikov – Ioffe Institute, 194021 St. Petersburg, Russia; St. Petersburg Electrotechnical University "LETI", 197022 St. Petersburg, Russia; ORCID 0000-0003-4345-6086; syncdima@mail.ru

Olga V. Proskurina – Ioffe Institute, 194021 St. Petersburg, Russia; St. Petersburg State Institute of Technology, 190013 St. Petersburg, Russia; ORCID 0000-0002-2807-375X; proskurinaov@mail.ru

Maria V. Tomkovich – Ioffe Institute, 194021 St. Petersburg, Russia; ORCID 0000-0002-1537-4107; maria.tom83@gmail.com

Valery L. Ugolkov – I. V. Grebenshchikov Institute of Silicate Chemistry of the Russian Academy of Sciences, 199034 St. Petersburg, Russia; ORCID 0000-0003-2895-0625; ugolkov.52@gmail.com

Victor V. Gusarov – Ioffe Institute, 194021 St. Petersburg, Russia; ORCID 0000-0003-4375-6388; victor.v.gusarov@gmail.com

Conflict of interest: the authors declare no conflict of interest.